June 2, 2008

First Year Summary: A First Look at the Vector Boson Fusion Higgs $\rightarrow \tau\tau$ Channel in ATLAS and Progress on the Forward Jet Trigger.

C. Taylor

Abstract

I report on the progress so far this year. The study of the VBF Higgs $\rightarrow \tau\tau$ channel has been my main analysis topic. This comprised of developing a cut-based selection to search for Higgs production in the low mass region, utilising the fully-leptonic final state produced by intermediate decay of the Higgs into τ leptons.
I also report on the ongoing work with the forward jet trigger. Until some months ago, jets with $|\eta| > 3.2$ were not reconstructed at trigger level in ATLAS. I have contributed to the validation of the new algorithms produced for these jets. Studies of diffractive physics (in earlier data runs) and VBF (later data runs) will greatly benefit on such forward jet triggering being available.

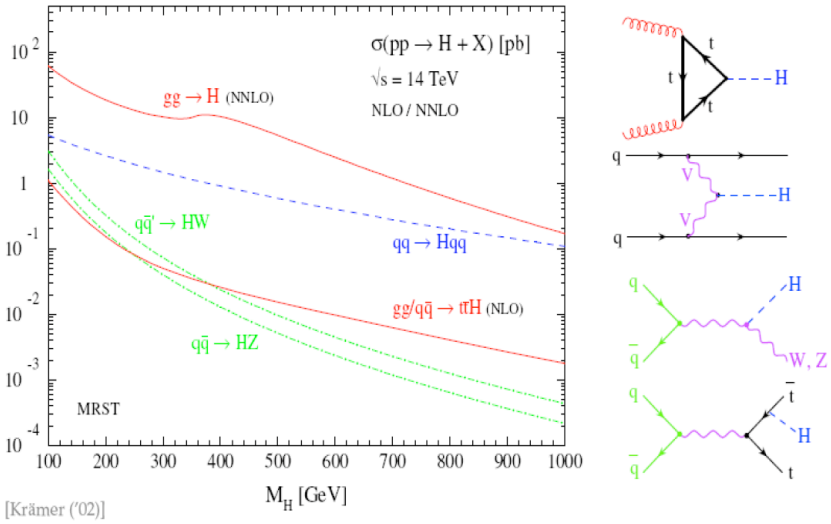

Figure 1: Relative production channel rates for the Higgs Boson.

1 Higgs Physics: Vector Boson Fusion

One of the main aims of the Large Hadron Collider (LHC) is to discover the source of electroweak symmetry breaking, the most viable candidate being the Standard Model Higgs Boson. At the LHC center of mass energy (14TeV), the most important channels of the Standard Model Higgs are shown in figure 1, and the main decay channels in figure 2. As can be seen from figure 1, Vector Boson Fusion production of the Higgs is a significant channel. From figure 2, $H \rightarrow bb$ is the main decay channel, but will suffer from a large QCD background. Therefore $H \rightarrow \tau\tau$ is a viable option for the low mass Higgs. As the Higgs mass increases, $H \rightarrow WW$ begins to dominate.

In a proton-proton collision that will be redolent with QCD events and interactions, the topology of the VBF Higgs to $\tau\tau$ channel has an unusual signature. As can be seen in the Feynmann diagram of figure 3, the vector bosons from the proton partons fuse to form the Higgs. The remnants of the quarks then hadronise into two jets in the forward part of the detector so these jets can be used as indicators that a VBF event has occured. The Higgs then decays to the two taus, which can then decay leptonically or hadronically. Taus decaying hadronically ($\tau \rightarrow \nu_\tau + n\pi$) will produce high p_T jets (ie highly collimated). Leptonic decay ($\tau \rightarrow \nu_\tau + e/\mu + \nu_{e/\mu}$) will produce either high p_T muons or electrons. For this report events that consist of purely leptonic decays have been considered, as a leptonic signal can be identified much more simply than a hadronic one in a proton-proton collision. Also, with only leptons in the final state and no colour flow between the forward-backward jets (as the Higgs is a colour singlet), there should be no high p_T jets in the central part of the detector, allowing a jet veto in this area.

The main background to this channel is a Z boson decaying to two leptons, faking the final state. The background becomes irreducable (apart from the reconstructed invariant mass) if the Z is also the product of vector boson fusion, as the forward jets will be mimicked. Other backgrounds include $W \rightarrow ee/\mu\mu$, $Z/W + Jets$, $t\bar{t}$, $W \rightarrow e/\mu/\tau + \nu_{e/\mu/\tau}$ and di-boson events.

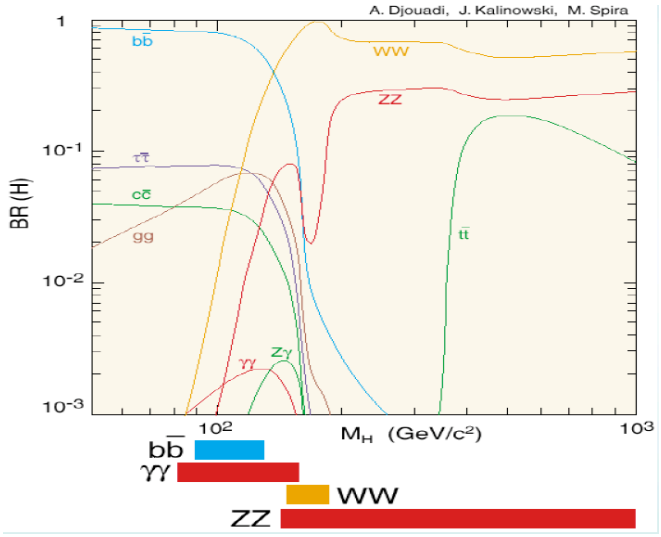

Figure 2: Relative decay rates of the Higgs Boson.

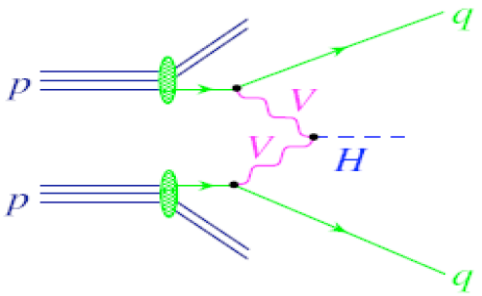

Figure 3: Feynmann Diagram of Vector Boson Fusion.

2 ATLAS and the LHC

The LHC is the next generation in a long line of colliders (figure 4), and it will operate at an unprecedented centre of mass(CoM) energy (14TeV), and luminosity. Constructed at CERN, it will collide 7TeV beams of protons every 25ns at different crossing points around the 27km ring at a depth of 50-175m. The detectors, A Large Toriodal ApparatuS (ATLAS), Compact Muon Solenoid (CMS), LHCbeauty (LHCb) and A Large heavy Ion Collider Experiment (ALICE), sit at these points. These energies will be achieved by injecting protons from the Proton Synchrotron (PS), then in the Super Proton Synchrotron (SPS) ring and then accelerating them using cryogenically cooled superconducting RF cavities operating at $2°K$. The foreseen design luminosity is $10^{34}cm^{-2}s^{-1}$. The LHC is due to start collisions in October 2008 at an initial CoM energy of 10TeV.

The main challenge of the LHC was to design and build the guiding magnets. These consist of superconducting dipoles operating at $2°K$ and 8.33T to confine the beam to the ring and also quadropoles to focus the beam. The dipoles are constructed from niobium-titanium coils with austenitic steel collars. [2]

ATLAS is a general purpose cylindrical detector composed of the tracker, electromagnetic and hadronic calorimeters (ECAL and HCAL), toroidal magnets and the muon

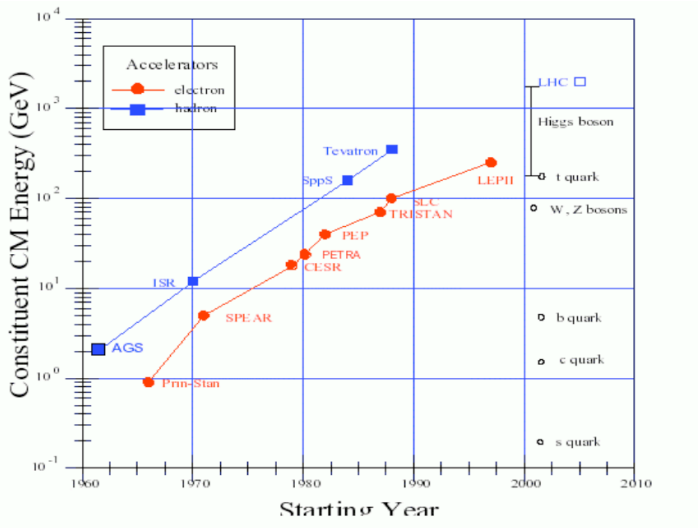

Figure 4: Centre of Mass energies progressing through time.

chambers around the barrel. The endcaps consist of forward calorimeters (FCAL) and muon chambers, as can be seen from figure 5.

The tracker is located in the inner detector, length 7m and radius 1.15m, and consists of discrete high-resolution semiconductor pixel and strip detectors, surrounded by continuous straw tube tracking detectors. A thin superconducting solenoid around the inner detector provides a magnetic field of 2T. This allows for pattern recognition, momentum and vertex measurements and electron identification. It has transition radiation capability in its outer part.

The calorimeters are contained within a cylinder with outer radius of 2.25m, and extends longitudinally to ±6.65m along the beam axis, and combined with the integrated iron magnet return yoke, weighs about 4000 tons. The ECAL consists of a highly granular liquid-argon (LAr) system, range $|\eta| < 3.2$, which allows excellent energy and position resolution. LAr is used for both EM and hadronic calorimeters in the endcaps, which extend coverage to $|\eta| < 4.9$. Most of the FCAL is provided by scintillator-tile calorimeters, seperated into a large barrel and two smaller extended barrel cylinders, giving good E_T^{miss} performance.

Around the calorimeters lies the muon spectrometer, which gives ATLAS its overall dimensions: radius 11m, half length of the barrel toroid coils is 12.5m, the high η muon detectors mounted on the cavern wall are 23m from the interaction point, and the overall weight is 7000Tons. Multiple-scattering effects are minimsed by the light and open structure and the large magnetic field volume, as well as the strong bending power provided by the toroid system and end-cap magnets. The toroid system consist of eight large superconducting independent air core toroids surrounding the calorimetry. Excellent muon momentum resolution is achieved with three stations of high-precision tracking chambers. The muon instrumentation also includes as a key component trigger chambers with very fast time response. [3]

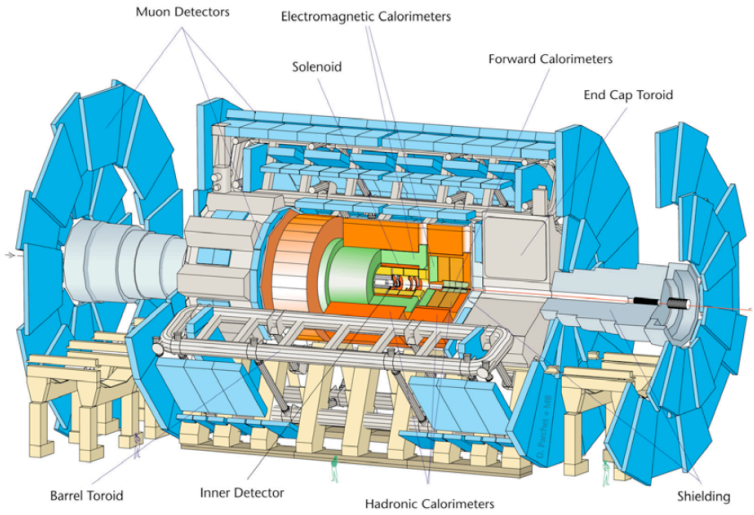

Figure 5: ATLAS Schematic.

3 The ATLAS Trigger: Forward Jet

When the LHC is running at full luminosity and the proton bunches are full, bunch crossings in ATLAS will occur at 40MHz. However, in each bunch crossing there will be an average of twenty interactions, giving a data rate of about 1GHz. As this would mean 1Pb/s of data in data acquisition (beyond the capacity to store of any concievable technology), a trigger system is needed to reject the vast number of channel hits with little physical significance. Therefore ATLAS has a three-tiered trigger system to reduce the data flow to 100Hz [4][5].

Level one is a hardware based trigger that must have timing performance as a primary concern, as it will have a latency of $2.5\mu s$. It uses the fast detectors (no tracker, only FCAL, HCAL, ECAL and muon chambers), has coarse granularity and low resolution and uses speciality hardware (FPGAs, some ASICs). It will output at a frequency of 75kHz, upgradeable to 100kHz.

Level two will confirm the Level one trigger and add tracking information, adding some simple event topology triggers. Full granularity and resolution will be available, and will operate on a farm of commercial processors with special algorithms. The acceptance and latency will be of order 1kHz and around 10ms respectively.

Lastly, the event filter will confirm level two, add topology triggers and perform a full event reconstruction. This will be run on a farm of commercial processors using near off-line code. The acceptance and latency will be 100Hz and around a few seconds respectively. Figure 6 demonstrates the the layout of the triggers and data acquisition.[6]

An important concept within the ATLAS trigger is the Region of Interest (RoI). This is a geometrical region of the ATLAS detector assigned by the level one trigger that may contain events of interest, and that should be investigated at higher trigger levels. A simple RoI description is via: $(\phi_{min}, \phi_{max}), (\eta_{min}, \eta_{max})$. The trigger assigns a word to such a region, which can be accessed at higher trigger levels.

The trigger system [7] is broken down into various slices, depending on the physical object it is triggering on. The jet slice is one of these, and at level one relies on

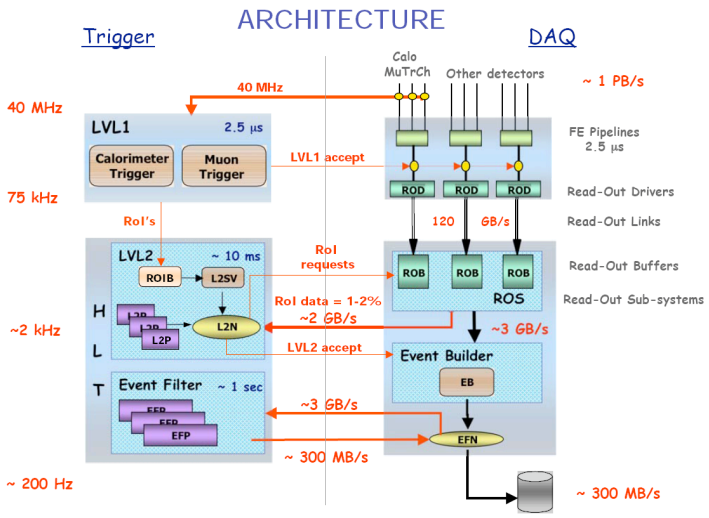

Figure 6: Trigger and DAQ architecture [6].

the calorimeter trigger processor. This produces electrons or photons, jets, taus, missing transverse energy and total transverse energy signatures. Trigger tower algorithms give EM and Hadronic information which provide an estimation of the energy collected by the calorimeter with a $0.1 \times 0.1(\eta \times \phi)$ granularity. These EM towers can be combined with neighbouring towers in η or ϕ, and also with their hadronic counterparts. For example a 2x1 trigger tower group would be two neighbouring towers at the same η or ϕ in the EM layer, with the same towers (directly behind) in the hadronic layer. The default for level one is a 4x4 trigger tower group.

Level two uses the RoI to begin the jet reconstruction. The RoI defines the centre of a grid in η and ϕ of calorimetry units with a given half-width. After this is read out, a simple cone jet algorithm is used. Starting from a jet defined as a cone of radius $R_{cone} = \sqrt{\Delta\eta^2 + \Delta\phi^2}$ from the RoI centre, an iterative procedure refines the jet position by recalculating the energy-weighted (η,ϕ)-position of the jet. Then a jet energy calibration tool improves the energy estimation of the jet.

At the Event Filter level, the jets may be reconstructed with either tower or topological cluster algorithms. Topological clusters, unlike towers, group calorimetry cells based on their neighbour relations and on the significance of their energy contents, producing clusters of variable cell numbers. Essentially, depending on whether towers or clusters are used, tower or cluster feature extraction algorithms are used after a general cell maker algorithm. Therefore jets can be reconstructed from towers or clusters, and either a cone or a fast Kt algorithm can be used[7].

4 VBF Analysis Results

To demonstrate the viability of this Higgs channel, it is first useful to show how the topology of a VBF event differs from background events. For this report a Higgs Mass of 120GeV was considered, decaying to a fully leptonic state, and three types of background were considered. Firstly, the QCD $Z- > \tau\tau + 1 < n < 5jets$, as this will have the greatest impact on the significance of the signal. Unfortunately due to technical

Process	Cross Section (pb)	No. of Events at $30fb^{-1}$
$H->\tau\tau->leptons$	0.022	660
$Z->ee+2jets$	5.99	179700
$Z->\tau\tau+1-5jets$	0.82	24510
$t\bar{t}$	461.160	13834800

Table 1: Cross-sections of the signal and backgrounds analysed for this report [8].

reasons, the electroweak part of this background could not be analysed. Although it has a cross section of O(100) smaller than the QCD, it will still contribute to the irreducible background. The long tail of the irreducible $Z->\tau\tau+1<n<5jets$ background has the possibility of swamping the Higgs signal. Secondly, a $t\bar{t}$ background was used. Although, as will be seen, this background can be well constrained with cuts, the magnitude of its' cross-section will create problems anyway. Lastly, a $Z->ee+2jets$ background is used. This is to demonstrate how the cuts employed can successfully deal with a background. Although the other backgrounds mentioned earlier in this report can be removed with cuts, they may still have an effect due to their cross-sections. Due to time constraints these could not be analysed in time for this report, and will be included in a later analysis.

As can be seen from the table of cross sections, 1, the Higgs cross-section is completely dwarfed by those of its backgrounds. Thus, without a system of cuts, this signal would never be seen. As the final state is purely leptonic (i.e. a high energy muon or electron), the e25i or mu20i triggers can be used. That is, an isolated electron or muon with energy 25 or 20 GeV respectively, which have an efficiency of around 9.0% [1]. Therefore there must be at least one lepton with a p_T equal to or greater than the trigger lepton. The final state can be exploited further, by requiring that there be exactly two leptons, and that they must have opposite charge (for charge conservation). The final state will also contain neutrinos, therefore a cut on the missing energy can be used (40GeV).

If the taus are indeed the daughters of a Higgs, due to the mass differences they should be boosted and highly collinear, as will the final state leptons. Therefore, as long as the two taus are not back to back (a cut on the $cos\phi$ between τs is used here), a collinear approximation can be used allowing a mass reconstruction even though some energy is removed via the neutrinos. This gives an equation of $M_{\tau\tau}=M_{ll}/(\sqrt{x_{\tau l1}x_{\tau l2}})$, where the x variables are the fraction of the τ momentum carried away by visible decay products. To ensure that the reconstruction remains physical and for good background rejection, the x variable are constrained to be within 0 and 0.75.

As stated before, the availability of tagging jets provides an excellent opportunity to suppress backgrounds due to their unique topology. As can be seen from figure 7, the VBF signal has the most fraction of events leading to two jets with a high pseudorapidity, compared to backgrounds $t\bar{t}$ and $Z->ee+2jets$. $Z->\tau\tau+1<n<5jets$ resembles the signal more than the other two, having low multiplicity forward jets, but not as great a fraction of them. This can also be observed in figure 14, where the signal has the greatest fraction of jets at high η. Figure 9 also shows that high p_T jets occur mainly within the forward regions of the detector. The lack of high p_T central jets motivates a central jet veto of these jets. The backgrounds have a greater chance of producing QCD radiation

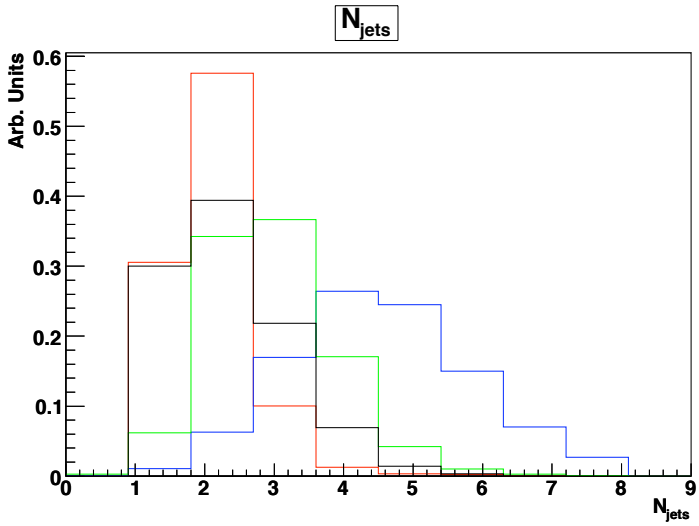

Figure 7: Number of jets of $\eta > 3.2$ per event for the signal. Red, blue green and black are Higgs, $t\bar{t}$, $Z- > ee + 2jets$ and $Z- > \tau\tau + 1 < n < 5jets$ respectively.

in the cenrtal part of the detector. These plots therefore motivate the following cuts: Firstly a requirement that a jet be found with a $p_T > 40GeV$, followed by a second jet of $p_T > 20GeV$. This selects a multiplicity of two jets. Next, a cut that selects the forward jets: $min\{\eta_{j1}, \eta_{j2}\} < \eta_{lep1,2} < max\{\eta_{j1}, \eta_{j2}\}$. This selects events where the η of the lepton system lies between that of the tagging jets. The central jet veto discards the event if a jet of $p_T > 20GeV$ falls within $|\eta| \leq 3.2$.

As can be seen from figure 10, the Higgs signal has a greater fraction of jets with a high $\Delta\eta_{jj}$ than any of the backgrounds, with $Z- > ee$ being the closest background. This motivates a simple cut on $\Delta\eta_{jj}$ of $\Delta\eta_{jj} > 4.4$. The signal event topology also requires that the jets be fairly collinear in ϕ. Therefore a constraint on $\Delta\phi jj$ of < 2.2 can be used. Figure 11 shows the invariant mass distribution of the jet system. As can be seen, the signal as a longer tail than the backgrounds (due to the high mass of the quark remnants, the forward jets). This motivates a cut of $M_{jj} > 700GeV$ on the invariant mass. To constrain the $t\bar{t}(+jets)- > l\nu bl\nu b(+jets)$, events that have b-tagged jets are vetoed. Because the tagging jets are fairly forward in the detector, the b-tagging requirement is rather loose [1].

The effect of the cuts described above have a rejection rate of order 10^8. Because of this, all backgrounds (except the irreducible $Z- > \tau\tau$) which in this study have Monte Carlo samples of order 10^5, equivalent to only a few fb^{-1}, have very low (if any) statistics after the cuts. Therefore a procedure is needed to estimate the background at the end of the analysis. This procedure is a cut factorisation method, which divides the cuts into three groups that are roughly uncorrelated. The first category consists of cuts that relate to the τ decays of the Higgs candidate. These include the trigger, lepton ID, Missing transverse energy, the collinear approximation and the transverse mass. The second category contains the cuts related to the tagging jets. These are the number of jets, forward jets, b-jet veto, $\Delta\eta_{jets}$ and M_{jets}. The third category consists of those which are strongly correlated to both forward tagging jets and tau decay products. These are the angular requirements,

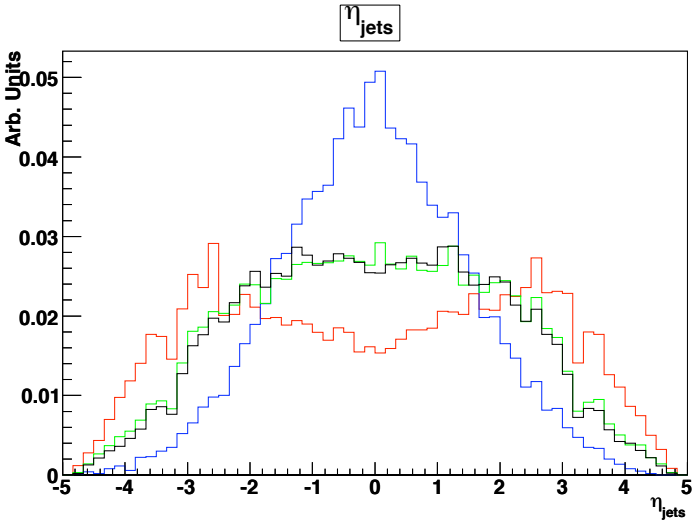

Figure 8: η_{jet} per event.Red, blue green and black are Higgs, $t\bar{t}$, $Z- > ee + 2jets$ and $Z- > \tau\tau + 1 < n < 5jets$ respectively.

centrality and the central jet veto. The method is quite simple: the rejection rate is calculated for the three categories seperately, and then the product is taken. This is then the estimation of the rejection rate of the whole analysis.

Normalising to the cross sections given in table 1, the $t\bar{t}$ is increased from having no events to 7.07 at $30fb^{-1}$. This can be combined with the signal and other backgrounds into a cut flow table, as shown in figure 12. Although this is a useful method for a low number of events, it does increase the uncertainty. Figure 12 shows the efficacy of the cuts mentioned previously on the signal and backgrounds. The numbers in italics are the product of the cut factorisation method. Even using this, it is not possible to gain a single $Z- > ee + 2jets$ event with the luminosity generated. Of particular interest is the Dilepton cut, which has a high rejection rate on both the signal and backgrounds. As this cut requires exactly two opposite charge leptons, one can surmise that there must be significant leptonic activity of high enough p_T to veto even signal events. As the bottom of the table is approached, the number of events decrease to the point where the statistical uncertainty will severely hamper any physical analysis.

After the cut process is complete, the remaining signal and backgrounds are presented in figure 13. The error bars have been omitted (simple statistical ones) as they dominate the plot due to the low number of events. A signal peak is clearly visible over the two backgrounds.

To calculate the significance, a mass window cut was imposed on the plot of 105-135GeV, to select the region of the Higgs signal. Then a simple counting experiment was used on the signal events (s) and the combined background events (b) [10]. A total of 5.61 signal events were counted, and 1.84 background events. Thus using $s/\sqrt{s+b}$, a significance of 2.06 was found for $30fb^{-1}$.

As this is a first look at the Vector Boson Fusion Channel, it is a fairly basic analysis, concentrating on one tau-tau decay system (the other two are the semi-leptonic and fully hadronic), but it does offer an idea of the importance of this channel for Higgs discovery

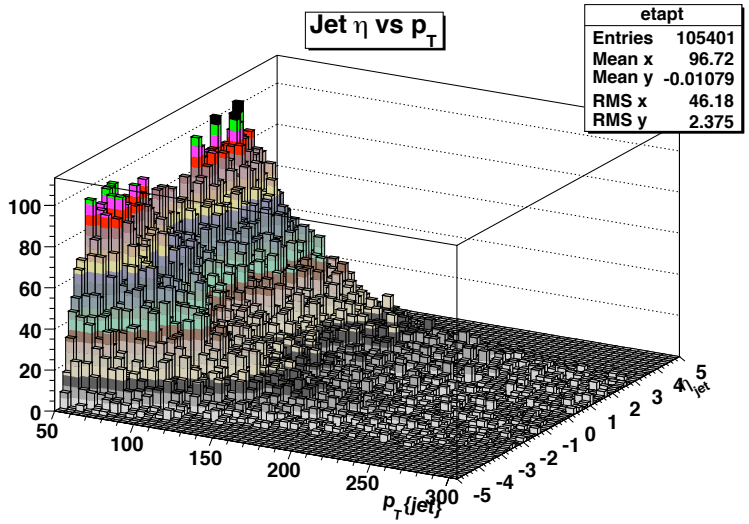

Figure 9: η_{jet} vs p_{Tjet}per event for the Higgs signal.A cut of 50GeV is in place to highlight the high η prevalence of high p_T jets.

at low Higgs mass. Issues to be considered in a future, more in depth analysis would be a proper treatment of the theoretical errors, systematic uncertainties and detector corrections, as well as performing the analysis on the backgrounds using a statistically useful luminosity. Unfotunately, producing the required amounts of Monte Carlo data provides technical difficulties. As the LHC turn-on is immenent, it may be useful to use the first low luminosity data to begin to understand some of the backgrounds. Also to be considered would be the effect of pile-up, which would increase hadronic activity in the central part of the detector. This would adversely affect the central jet veto, generally degrading the missing transverse energy resolution, and therefore degrade the mass reconstruction. It would be useful to use more complex statistical methods as in [1] to calculate the significance, and mass resolution, as well as analyse some of the efficiencies of various cut algorithms.

5 Trigger Results

As stated in the abstract, until recently there existed no forward jet trigger at Level two or Event Filter. Level one existed, but had no segmentation in the endcap, thus no η granularity was available. Certain physics studies, such as diffractive physics and VBF have jets with a high η value as part of their event signature. Therefore it is useful to have a more efficient forward trigger. An algorithm was recently encoded to unpack the FCAL, which has to be validated before it can become part of the ATLAS trigger system.

To validate this software, it first seemed appropriate to check that the software was indeed reconstructing jets in the forward region. As can be seen from figure 14, jets are indeed present at $\eta > 3.2$ at the event filter level, as well as L1 and L2 compared to truth. The dataset used was an Invisible Higgs set generated by M. Schram, producing an ntuple to use of 10k events. The jets were also present in the level two and level one triggers.

Next, it is useful to compare the efficiency of the new trigger. This was done by constructing the EF jets before the level 1 and 2 triggers, and then constructing them

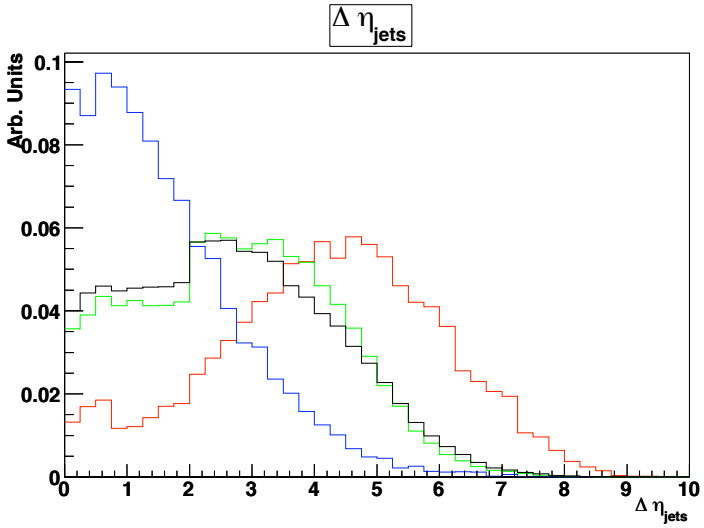

Figure 10: $\Delta\eta_{jets}$ per event.Red, blue green and black are Higgs, $t\bar{t}$, $Z- > ee + 2jets$ and $Z- > \tau\tau + 1 < n < 5jets$ respectively.

again (looping over the events and using RoI matching), and taking the ratio. The jets were split up into forward $\eta > 3.2$ and central $\eta < 3.2$ jets, and a cut of 18GeV or 40GeV on the transverse energy was applied. As can be seen from figures 16 and 15, the effiencies are comparable. This suggests that the foward and central jet reconstructions have a similar performance.

The next part of the validation was to look at the η and ϕ resolutions of the jet reconstruction relative to different trigger levels. This was done by using RoI word matching of jets at different levels, and taking $\Delta\eta$ and $\Delta\Phi$ between the levels. This was done for the forward and central jets seperately, and comparing 1-2, 1-EF and 2-EF trigger levels. In figures 17 and 18, central jets are black, forward jets are red. As can be seen from figure 17, forward jet 1-2 level resolution performs poorly compared to the central jet. This is due to the poor granularity at level 1 in the forward region, and possibly a reconstruction problem at level two of the forward jets. Level 1 - EF also performs poorly compared to central jets, having no spread peak at zero indicating correctly matched jets. Between level two and EF performance is similar, though suffering from poor statistics. In figure 18, forward jets again has a worse resolution, but less so, and is slightly better in 1-3. Performance is similar between 2-3.

Lastly, it is very important that the new algorithm acts within the time constraints of the trigger software during runing. This will be especially important when the LHC runs at the design luminosity with completely filled bunches. Therefore, the timing of the jet reconstruction is needed. Figure 19 shows the speed of the algorythm compared to the η of the jet. As can be seen, forward jets are on average quicker than than central jets, meaning this algorithm can be used in the ATLAS trigger.

As a final note, the code was was also checked for memory leaks using the Valgrind tool. Although memory leaks were found, they were found to be caused by the athena framework.

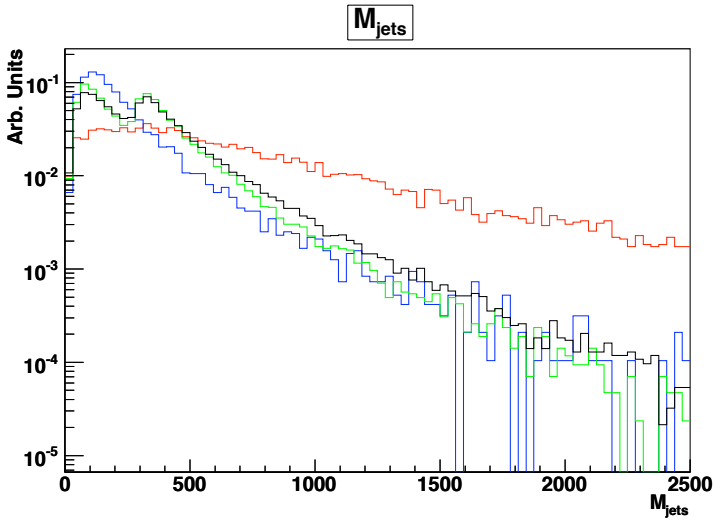

Figure 11: M_{jets} per event.Red, blue green and black are Higgs, $t\bar{t}$, $Z- > ee + 2jets$ and $Z- > \tau\tau + 1 < n < 5jets$ respectively.

References

[1] Search for the SM Higgs boson via Vector Boson Fusion production process in the d-tau channels with ATLAS (Draft), ATLAS Collaboration, April 4, 2008

[2] LHC Design Report, Accelerator and Beam Division, 2 March 2004

[3] Technical Design Report - Chapter 1 Overview Letter, ATLAS Collaboration, 25 May 1999, ATLAS TDR 14, CERN/LHCC 99-14

[4] The ATLAS Trigger, Rainer Stamen, 24 November 2005

[5] Technical Design Report - Chapter 11 Trigger Performance, ATLAS Collaboration, 25 May 1999, ATLAS TDR 14, CERN/LHCC 99-14

[6] London HEP Postgraduate Lecture Course - Trigger and DAQ, November 2007, Fred Wickens

[7] TrigJetOverview - Twiki, 18 October 2007, Cibran Santamarina Rios

[8] VBFHTauTau - Twiki, 20 May 2008, Soshi Tsuno

[9] Pythia 6.4 Physics and Manual, Torbjorn Sjostrand, Stephen Mrenna, Peter Skands,March 2006, hep-ph/0603175

[10] Particle Data Group, W.-M. Yao et al., J. Phys. G 33, 1 (2006)

	Higgs->tautau	Z->tautau+njets	ttbar	Z->ee+2p
Total events	660	24510	13834674	179768
Trigger (Passed_EF_e25i==1)	659.98	24510.06	13834674	179700.04
Lepton (thisElectron==1)	184.32	6214.26	2948493.96	142649.98
Trigger lepton (trigLepPt > 25GeV)	150.73	4825.63	2475353.32	127867.96
Dilepton (thisDilepton == 1)	71.4	2830.92	323144.04	64275.06
Opposite charge leptons (thisOppositeSign == 1)	71.09	2818.45	313317.96	63761.05
Missing energy (MET_RefFinal_et > 40GeV)	49.51	1918.16	272152.64	45328.98
Collinear approx. (tauDau1X > 0.0)	49.51	1918.16	272152.64	45328.98
Collinear approx. (tauDau1X < 0.75)	33.48	1072.08	211186.28	634.32
Collinear approx. (tauDau2X > 0.0)	33.02	1051.61	143445.88	582.37
Collinear approx. (tauDau2X < 0.75)	27.79	888.72	89476.88	131.24
Collinear approx. (tauDauCosdphi > -0.9)	27.17	852.71	57244.36	113.47
Collinear approx. (dPhill < 2.2)	23.85	707.06	46971.64	58.78
N jets ≥ 2 (jet1Pt > 40GeV)	23.1	690.8	25458.48	31.44
N jets ≥ 2 (jet2Pt > 20GeV)	19.31	400.06	11910.4	15.04
Forward jet (thisForwardJet == 1)	17.91	218.48	4764.16	8.2
Centrality (thisCentrality == 1)	16.56	187	4094.2	4.1
B-jet veto (thisBjetVeto)	15.81	180.53	2828.72	1.37
Delta eta of jets (deltaEtajj > 4.4)	13.51	148.89	1116.6	1.37
Delta phi of jets (dPhijj < 2.6)	8.66	31.64	372.2	1.37
Inv. Mass of jets (Mjj > 700GeV)	7.39	18.37	372.2	0
Central Jet Veto (thisCentralJetVeto == 1)	6.28	8.9	*7.07*	*0.00402*

Figure 12: Events remaining after each cut, normalised to the cross-sections in figure 1. The values in italics have been approximated using the cut factorisation method.

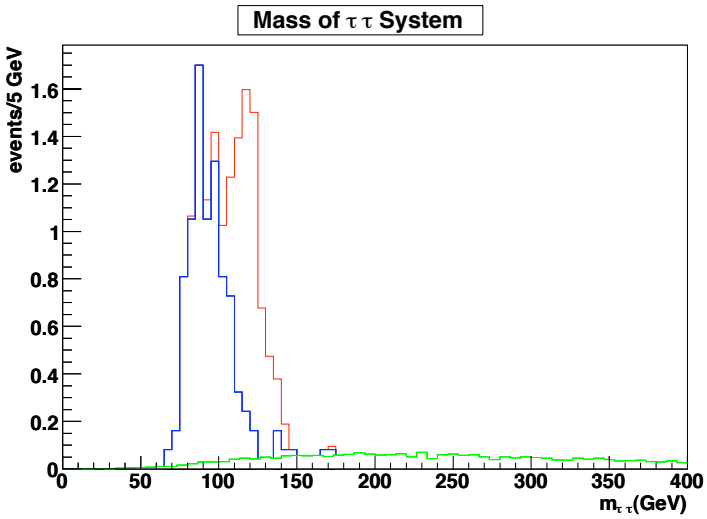

Figure 13: Mass of the $\tau\tau$ system, normalised to $30fb^{-}1$.Red, blue and green are Higgs,$Z- > \tau\tau + 0 < n < 5jets$ and $t\bar{t}$respectively.

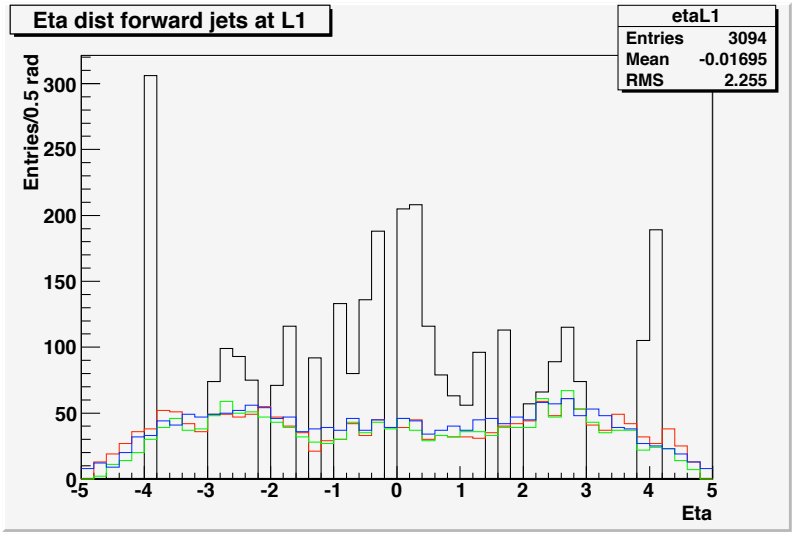

Figure 14: η_{jet} at L1 (black), L2 (red), EF (green) and truth (blue).

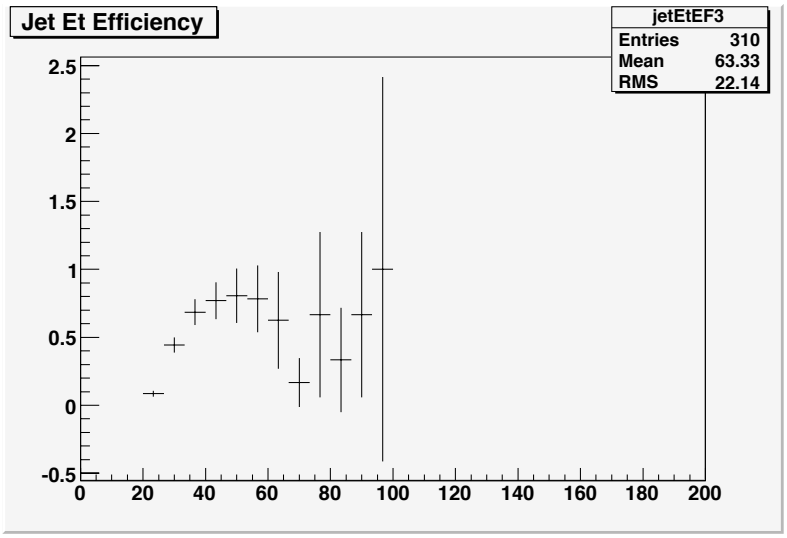

Figure 15: Event Filter reconstruction efficiency of forward jets with an 18GeV cut.

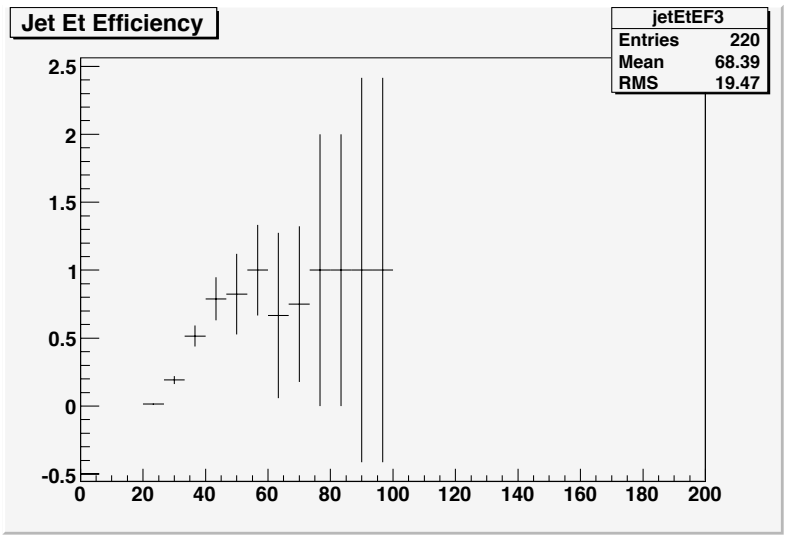

Figure 16: Event Filter reconstruction efficiency of central jets with an 18GeV cut.

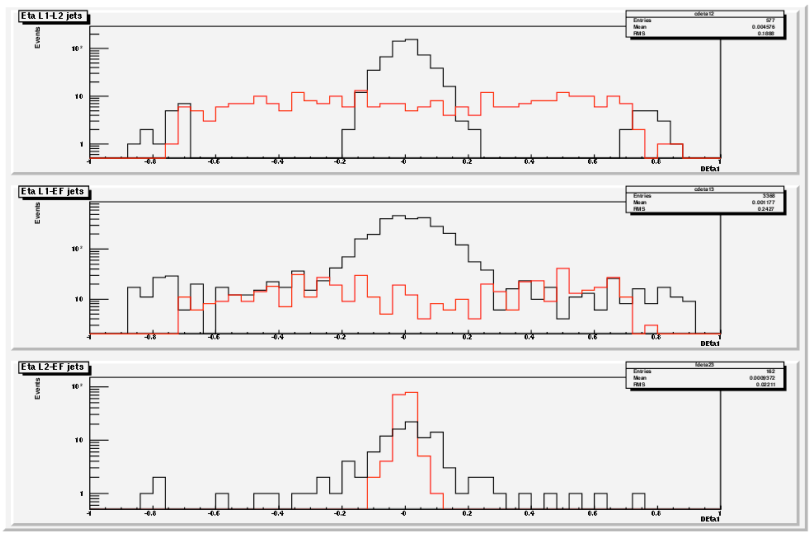

Figure 17: $\Delta\eta$ between trigger levels for forward and central jets.

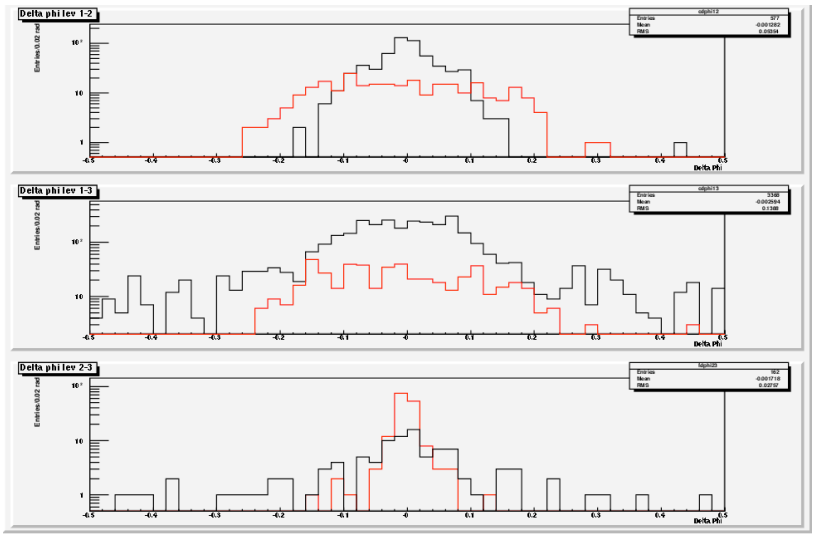

Figure 18: $\Delta\Phi$ between trigger levels for forward and central jets.

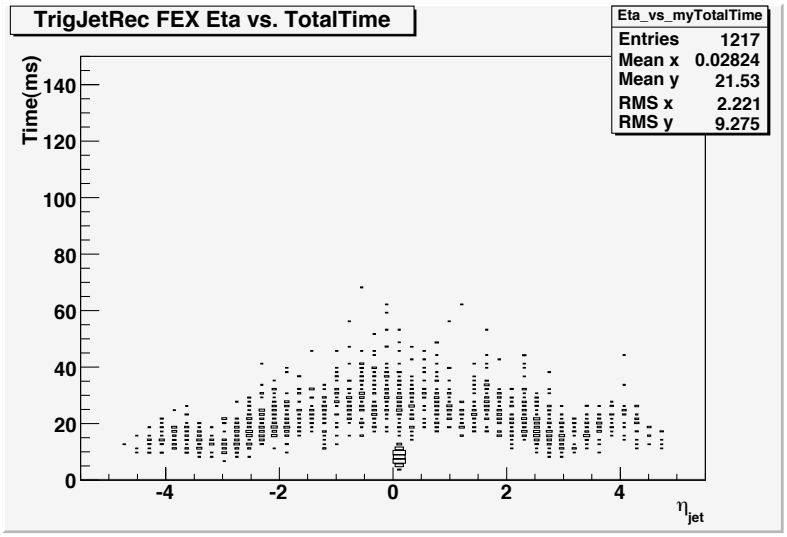

Figure 19: Time for trigger to reconstruct vs η of jets.